Materiales de Construcción
Vol. 69, Issue 336, October–December 2019, e200
ISSN-L: 0465-2746
https://doi.org/10.3989/mc.2019.12918

Effect of different PVA and steel fiber length and content on mechanical properties of $CaCO_3$ whisker reinforced cementitious composites

M. Cao, C. Xie✉, L. Li, M. Khan

School of Civil Engineering, Dalian University of Technology, Liaoning (People's Republic of China)
✉xie_chaopeng@mail.dlut.edu.cn

Received 26 November 2018
Accepted 9 May 2019
Available on line 25 September 2019

ABSTRACT: In this paper, calcium carbonate ($CaCO_3$) whisker as a fiber reinforcement is mixed with steel and PVA fiber to form a multiscale hybrid fiber reinforced cementitious composites (MHFRCC). ASTM standard and post-crack strength techniques are performed to evaluate the mechanical properties of MHFRCC. The 1.25 % long steel fiber, 0.55 % short PVA fiber and 2.0 % $CaCO_3$ whisker specimens showed the best flexural behavior before L/600 deflection. However, 1.5 % long steel fiber, 0.4 % long PVA fiber and 1.0 % $CaCO_3$ whisker specimens presented better crack resistance after L/600 deflection. It is revealed that flexural parameters increase as comprehensive reinforcing index increase. The result showed that the $CaCO_3$ whisker and short PVA fiber provided crack resistance effect at micro-scale and mainly play a dominate role in inhibiting microcracking. However, long steel fiber and long PVA fiber showed a better bridging effect of macro cracks at a large deflection.

KEYWORDS: Composite; Calcium carbonate; Fiber reinforcement; Mechanical properties; Microcracking.

Citation/Citar como: Cao, M.; Xie, C.; Li, L.; Khan, M. (2019) Effect of different PVA and steel fiber length and content on mechanical properties of $CaCO_3$ whisker reinforced cementitious composites. Mater. Construcc. 69 [336], e200 https://doi.org/10.3989/mc.2019.12918

RESUMEN: *Efecto de diferentes tamaños y contenidos de fibras de PVA y acero en las propiedades mecánicas de materiales cementantes compuestos reforzados con filamentos de $CaCO_3$.* En este estúdio, filamentos de carbonato de cálcio ($CaCO_3$) se han empleado como fibras de refuerzo junto com fibras de acero y PVA, com el fin de producir un material cementiceo compuesto híbrido fibrorreforzado (MHFRCC). Para evaluar las propriedades mecánicas de estos materialess, se han empleado normas ASTM y técnicas de resistencia post-fisuración. La mezcla con mejor comportamento a flexión hasta el valor de flecha L/600 fue la compuesta por 1,25% de fibra larga de acero, 0,55% de fibra corta de PVA y 2,0% de filamento de $CaCO_3$. Sin embargo, la mezcla con 1,5% de fibra larga de acero, 0,4% de fibra corta de PVA y 1,0% de filamento de $CaCO_3$ presentó la mejor resistencia a fisuración tras el valor de flecha L/600. Se há visto que los parámetros de flexión aumentan al incrementarse el índice de refuerzo. Los resultados muestran que los filamentos de carbonato cálcio y las fibras cortas de PVA aportan restistencia a fisuración a nível de microescala, jugando um importante papel inhibiendo la formación de micro-fisuras. Sin embargo, las fibras largas de acero y de PVA mostraron um mejor efecto puente em las macro fibras tras uma mayor flecha.

PALABRAS CLAVE: Materiales compuestos; Carbonato de calcio; Refuerzo de fibras; Propiedades mecânicas; Microfisuración.

ORCID ID: M. Cao (http://orcid.org/0000-0002-7917-4710); C. Xie (https://orcid.org/0000-0003-4544-5954); L. Li (http://orcid.org/0000-0003-3966-6363); M. Khan (http://orcid.org/0000-0003-2898-1827)

1. INTRODUCTION

The inherent brittle behavior of cementitious composites leads to a low tensile strength, toughness, impact resistance and cracking (1–3). Therefore, fibers are added to enhance the crack resistance, tensile strength and ductility of fiber reinforced cementitious composites(FRCC)(3,4).The hybrid fiber system with multi-scale characteristics is widely used to reinforce cementitious composites. In comparison with normal FRCC, hybrid fibers can make the effect of toughening and strengthening at multi-level (5,6). Usually, long fibers and short fibers are mixed together in FRCC for controlling cracking at different levels (7–11). However, the metallic fiber, polymeric fiber or natural fiber only can restrict macroscopic or mesoscopic cracks in cementitious composites. Therefore, it is necessary to add a low cost microscale fiber to arrest cracks at microscale.

$CaCO_3$ whiskers (CW) is an inorganic microfiber like needle having characteristic of high strength, high elastic modulus, low price (approximately U.S.$230 per ton), large aspect ratio and better crack resistance at micro level (12–13). Cao et al. (12) added CW into cement-based materials firstly and CW could effectively restrict the generation and propagation of cracks at microscopic level. Cao et al. (13) also reported that adding CW into cement mortar not only improved the compressive and flexural strength of cement mortar but also enhanced the flexural toughness. Furthermore, the microstructure of CW could fill the pores of cement mortar and make it denser. On the other hand, the behavior of whisker pullout, crack deflection, whisker bridging and whisker breakage could increase flexural performance. Thus, CW may be one of the ideal reinforced material at microscale in cementitious composites. Zhang et al. (14) and Cao et al. (15–18) studied CW into PVA-steel fibers reinforced cementitious composites to form a multiscale hybrid fiber reinforced cementitious composites (MHFRCC). The result showed that both compressive strength and flexural performance of MHFRCC are significantly improved showing the multiple cracking behavior.

Flexural behavior is an important mechanical behavior of FRCC influenced by many material parameters, such as strength, elastic modulus of matrix, fiber length, type, content, dispersion and interaction between fiber and matrix (11, 19). Therefore, large numbers of researchers have focused on studying the material parameters of FRCC to minimize cost and maximize flexural behavior of FRCC. Kim et al. (19) compared the flexural performance of four fibers (twisted steel, hook steel, polyethylene spectra and polyvinyl alcohol) in reinforced cementitious composites. The matrix consisting of twisted steel fibers showed best flexural behavior of equivalent flexural strength, flexural toughness and multiple cracking behaviors. However, matrix with PVA fiber presented the worst flexural performance as compared to that of other fiber reinforced cementitious composites without PVA fiber. The result indicated that different fiber type and fiber length have prominent impact on flexural behavior of FRCC. Banthia and Soleimani (7) investigated the flexural performance of hybrid fiber reinforced concrete. The result showed that combination of steel and polypropylene fiber reinforced concrete (SPFRC) has higher post-cracking strength (PCS) value than that of single steel fiber reinforced concrete (SFRC). However, the addition of mesophase carbon fiber to SPFRC showed a higher PCS value as compared to that of SPFRC. It was found that there existed synergistic effect among steel fiber, polypropylene fiber and carbon fiber.

The flexural behavior of cementitious composites is mainly determined by many parameters and the interaction between fiber and matrix. Thus, different fiber type, length and content should be studied in depth to minimize cost and maximize flexural behavior of FRCC. To the best of author's knowledge, no study has been reported on flexural behavior of MHFRCC with combination of calcium carbonate whisker, PVA fiber and steel fiber having various type, content and length. Thus, two type of steel fibers (short steel fiber(SS)and long steel fiber (LS)), two lengths of PVA fibers (short PVA fiber (SP) and long PVA fiber(LP)) and CW are considered to form different MHFRCC. The purpose of this study is to explore the effect of steel-PVA fiber lengths and contents on the overall flexural performance of $CaCO_3$ whisker reinforced cementitious composites. Thus, many tests were employed to characterize the measured physical properties of MHFRCC. The mechanical parameters of the MHFRCC are investigated to determine the influence of steel fibers, PVA fibers and CW at different flexural stages.

2. FLEXURAL PARAMETERS OF MULTISCALE HYBRID FIBER REINFORCED CEMENTITIOUS COMPOSITES

The flexural behavior of MHFRCC was evaluated by different flexural parameters according to ASTM standards (20–21), post-crack strength (*PCS*) (1, 22-23) and reinforcing index (*RI*) (22-25).

2.1. ASTM standards

The point that becomes first nonlinear on the load-deflection curves is taken as the first cracking point according to ASTM C1018.The first-crack strength, deflection and toughness are important parameters to evaluate pre-cracking behavior. The peak-load point of load-deflection curve described in ASTM C1609 is another important point and its

corresponding peak strength, deflection and toughness are used to evaluate flexural behavior (11, 19). Furthermore, the residual strength and flexural toughness at specific point such as 600/span, 150/span are also used to analyze the flexural behavior of MHFRCCs in this study (21). Besides this, the 100/span point is further studied to describe the flexural behavior of MHFRCC (11, 19). The schematic diagram of these specific points is shown in Figure 1.

The flexural toughness is the energy absorption capacity of the test samples and can be obtained by calculating the areas under the load-deflection curve up to a specified deflection. The values of strength at these specific points are used in the following Equation [1] according to ASTM C1609/1609M-12.

$$f = \frac{PL}{bh^2} \quad [1]$$

Where f is the strength at specific point; P is the applied load at these specific points; b and h are the width and height of specimen, respectively.

2.2. Post-crack strength technique

The flexural toughness could be obtained through two standard methods, i.e. ASTM C1018 and JSCE-SF4. However, Banthia and Trottier (1) reported thatASTM C1018 and JSCE-SF4 test methods have some imperfection. The main problem of these two test methods was discussed and their susceptibility to human judgment errors was shown. The calculation of toughness index requires an accurate location of first cracking point but ASTM C1018 standard has occasionally in determining the location of first crack point. Similarly, the deflection point of span/150 which described in JSCE- SF4 is always be criticized for having higher value than that of acceptable deformation limit. Based on above reasons, post-crack strength (*PCS*) technique was proposed to evaluate the flexural toughness of FRCC. The schematic diagram of *PCS* technique is shown in Figure 2 and is calculate by Equation [2] and Equation [3].

$$PCS = \frac{E_{post,m} \cdot L}{\left(\frac{L}{m} - \delta_{peak}\right) bh^2} \quad [2]$$

$$E_{post,m} = E_{total,m} - E_{pre} \quad [3]$$

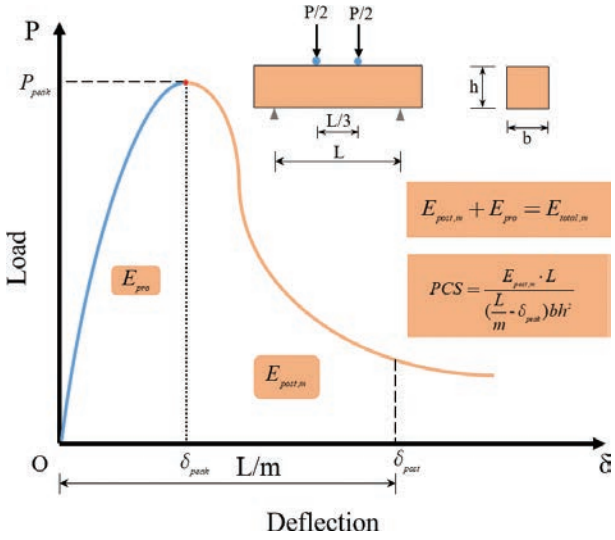

FIGURE 2. The schematic diagram of PCS technique.

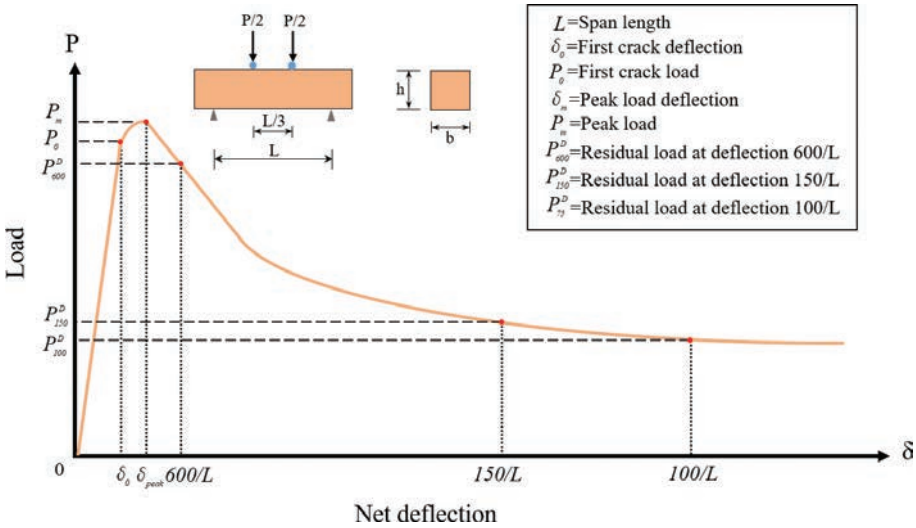

FIGURE 1. Schematic diagram of specific points according to ASTM.

Where $E_{post,m}$ is equal to the total energy ($E_{total,m}$) minus the pre-peak energy (E_{pre}); L is span length of specimen; δ_{peak} is the value of deflection at ultimate load; the value of m can be chosen on the basis of the considered application. Where b and h are the width and height of the specimen, respectively.

2.3. Reinforcing index

The fibertype, lengthand content are significant factors for evaluating the cracking behavior of FRCC. Ezeldin and Balaguru (26) proposed the reinforcing index to evaluate the effect of hooked end steel fiber in concrete. Then reinforcing index was extended to evaluate the effect of other type of steel fiber in concrete (22, 23, 27). CECS38:2004 (28) defined a characteristic value of steel fiber which had relationship with fiber content and aspect ratio. However, these stipulations were only for one type of fiber and could not be applied to hybrid fibers. Meanwhile, the simple superposition method of reinforcing index for each fiber is not a good choice because different fibers present different characteristics. Thus, a comprehensive reinforcing index(RI_v) was developed to describe the effect of hybrid fiber system (24, 25, 29). The formula of comprehensive reinforcing index is presented as follow in Equation [4]:

$$RI_v = \sum_i^n k_i v_{fi} \frac{l_i}{d_i} \left(\frac{f_i}{f_s} \right)^m \quad [4]$$

Where RI_v is comprehensive reinforcing index of hybrid fiber and k_i is the mechanical anchoring coefficient between fiber and matrix. In this study, SSF, SPF, LPF and CW are taken as 1, and HSF is taken as 1.66 (28). The v_{fi}, l_i, d_i represent the fiber content, fiber length and fiber diameter, respectively. f_i is the tensile strength of different fiber type and f_s is the tensile strength of steel fiber. The m is fiber type index, and for steel fiber it is 1and for PVA fiber and CW both are taken as 0.5 (29).The suffix i represent different fiber type. The value of i is taken as 1, 2 and 3 for steel fiber; PVA fiber and CW, respectively.

3. EXPERIMENTAL PROGRAM

3.1. Materials

The raw materials were Portland cement (P·O 42.5R), silica sand, ordinary tap water and superplasticizer. The chemical compositions of cement is shown in Table1. The physical properties and mix proportion of matrix are presented in Table 2. The water/ cement ratio was kept as 0.3, and sand/ cement ratio was controlled to 0.5 according to previous study (16, 18).The superplasticizer of 0.5wt %-1.5wt% was used to ensure workability of fresh mixture because of addition of PVA-steel fibers and $CaCO_3$ whisker. The steel fibers were from Bekaert Co. and PVA fibers were acquired from Wanwei High-Tech Material Co. (Chaohu, China). The $CaCO_3$ whiskers were provided by Youxing Technology Co. (Changde, China), and their chemical composition is also shown in Table 1.The appearance of these fibers are shown in Figure 3. The mechanical properties of these fibers were provided by manufacturer and are presented in Table 3.

The previous findings (16) showed that 1.5 vol % of steel fibers, 0.5 vol % of PVA fibers and 1.0 vol % of $CaCO_3$ whiskers and 1.25 vol % of steel fibers, 0.55 vol % of PVA fibers and 2.0 vol % of $CaCO_3$ whiskers had a better flexural behavior for MHFRCC. Therefore, these two fiber contents are selected in this study and the detailed mix proportions of $CaCO_3$ whisker-PVA-steel fiber are shown in Table 4.

Table 1. Chemical compositions of cement and $CaCO_3$ whiskers (wt. %).

Composition	CaO	SiO_2	Al_2O_3	Fe_2O_3	CO_2	MgO	K_2O	SO_3	Na_2O	P_2O_5	MnO
Cement	61.13	21.45	5.24	2.89	2.37	2.08	0.81	2.50	0.77	0.07	0.06
Whisker	54.93	0.29	0.11	0.07	42.07	2.14	-	0.31	-	-	-

Table 2. Raw materials properties and Matrix mix proportion.

Materials name	Density (g/cm^3)	Properties	Matrix proportion
Cement	3.2	Specific surface area 356m^2/kg Origin: Dalian Onoda cement	1
Water	1.0	Origin: Tap water	0.3
Silica sand	2.65	Fineness modulus 1.9 Moh's hardness 7	0.5
Superplasticizer	-	water-reducing ratio24.1% Origin: Sika Co. Ltd.	0.5%–1.5%

FIGURE 3. The fibers used in this study: Short steel fiber (SS); Long steel fiber (LS); Short PVA fiber (SP); Long PVA fiber (LP); $CaCO_3$ whisker (CW); SEM of CW.

TABLE 3. The physical properties of steel fiber, PVA fiber and $CaCO_3$ whisker.

Fiber type	Length (mm)	Diameter (μm)	Density (g/cm^3)	Tensile strength (MPa)	Elastic modulus (GPa)
Short steel fiber	13	200	7.80	2850	210
Long steel fiber	35	550	7.80	1345	210
Short PVA fiber	6	39.7	1.30	1259.5	36.7
Long PVA fiber	12	39.7	1.30	1259.5	36.7
$CaCO_3$ whisker	0.02–0.03	0.5–2.0	2.86	3000–6000	410–710

3.2. Mixing, casting and test procedure

Model HJW-60 concrete blender was used to mix the raw material. First of all, Portland cement, silica sand and CW were added into blender and rotated for about 30 seconds to ensure homogeneity of dry material. Secondly, water blended with superplasticizer were divided into three parts and poured into mixer three times during next 60seconds mixing. The fibers were added gradually until the mortar showed a good workability. Since PVA fiber was easier to agglomerated than steel fiber, so the sequence of addition was steel fiber followed by PVA fiber. To ensure the dispersion, steel fiber was divided into three parts and added into mortar for three times during next 120 seconds. Then, PVA fiber was gradually added

TABLE 4. Mix proportions of fibers.

Group		Volume fraction/%			Fiber dosage/(kg/m^3)		
		Steel fiber	PVA fiber	$CaCO_3$ whiskers	Steel fiber	PVA fiber	$CaCO_3$ whiskers
Control	Plain	0	0	0	0	0	0
Control-I	SS2.0	2.0	0	0	156	0	0
Series-I	SS1.5SP0.5	1.5	0.5	0	117	6.50	0
	SS1.5SP0.4CW1.0	1.5	0.4	1.0	117	5.20	28.6
	SS1.25SP0.75	1.25	0.75	0	97.5	9.75	0
	SS1.25SP0.55CW2.0	1.25	0.55	2.0	97.5	7.15	57.2
Series-II	SS1.5LP0.5	1.5	0.5	0	117	6.50	0
	SS1.5LP0.4CW1.0	1.5	0.4	1.0	117	5.20	28.6
	SS1.25LP0.75	1.25	0.75	0	97.5	9.75	0
	SS1.25LP0.55CW2.0	1.25	0.55	2.0	97.5	7.15	57.2
Control-II	LS2.0	2.0	0	0	156	0	0
Series-III	LS1.5SP0.5	1.5	0.5	0	117	6.50	0
	LS1.5SP0.4CW1.0	1.5	0.4	1.0	117	5.20	28.6
	LS1.25SP0.75	1.25	0.75	0	97.5	9.75	0
	LS1.25SP0.55CW2.0	1.25	0.55	2.0	97.5	7.15	57.2
Series-IV	LS1.5LP0.5	1.5	0.5	0	117	6.50	0
	LS1.5LP0.4CW1.0	1.5	0.4	1.0	117	5.20	28.6
	LS1.25LP0.75	1.25	0.75	0	97.5	9.75	0
	LS1.25LP0.55CW2.0	1.25	0.55	2.0	97.5	7.15	57.2

Note: SS represent smooth straight steel fiber; LS represent long steel fiber; SPre present short PVA fiber; LPre present long PVA fiber; Series-I represent fiber combination of (SS+SP); Series-II represent fiber combination of (SS+LP); Series-III represent fiber combination of (LS+SP); and Series-IV represent fiber combination of (LS+LP).

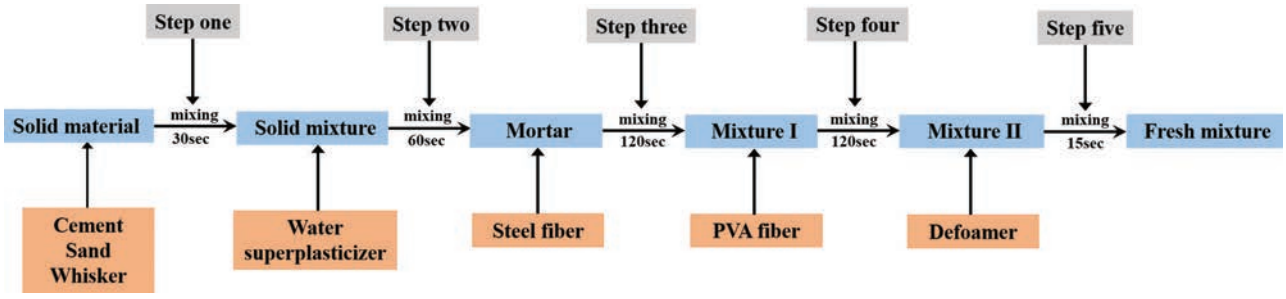

FIGURE 4. Flow chart of mixing process.

and mixed for next120 seconds, so that dispersion can be improved and agglomeration can be reduced. Finally, defoaming agent (10 ml tributyl phosphate) was added into mixture and blended for another 15 seconds to eliminate the bubbles caused by addition of fibers and whiskers. The flow chart of mixing process of raw materials is shown in Figure 4.

After that, fresh mixture was carefully placed in the middle of plastic molds one time by a spoon to let fresh mixture flow from the middle to both ends of plastic molds. The molds were then put on vibrator for 30 seconds to improve compactness of fresh mixture which guarantee the consolidation between fibers and mortar (30). Three specimens were casted from each mixture. Later, all the specimens were covered with plastic sheet and placed at laboratory temperature. After 24 hours, the specimens were demolded and cured for 28 days at 20±2°C temperature with more than 95% relative humidity according to GB/T 50081-2002 (31).

The dimension of beam was 100 mm × 100 mm × 400 mm for performing flexural properties. At the same

time, 100 mm × 100 mm × 100 mm cubes were also cast for testing compressive strength according to CECS13:2009(30). Before testing, two-line displacement sensors GA-10 (LVDT) made in Beijing King Sensor Technology Co. Ltd. were fixed with a special device to measure mid-span deflection on both sides of specimen. The application of this special device could avoid additional deformations came from support, loading points and twisting of the specimen. The BLR-1/10T load cell was employed to measure load value. The four-point flexural test was performed to determine flexural parameters of beams by electro-hydraulic servo universal testing machines. The displacement control method with a loading rate of 0.05mm/min according to ASTM C1609. The testing data were collected using DH3820 high speed static strain test analysis system at 5 Hz. The loading setup of beam is shown in Figure 5 and the schematic diagram of data collection is presented in Figure 6.

4. RESULT AND ANALYSIS

4.1. Compressive strength

The compressive strength of MHFRCCs are presented in Table 5 and Figure 7. It can be seen that samples cosisiting of fibers showed a higher compressive strength than that of plain sample. In comparison with plain group, compressive strength of SS2.0 and LS2.0 were increased by 39.27% and 11.58%, respectively. The increasement values in compressive strength can be attributed to crack resistance effect of steel fibers in cementitious composites. The compressive strength of SS1.5SP0.5, SS1.25SP0.75, SS1.5LP0.5 and SS1.25LP0.75 were reduced by

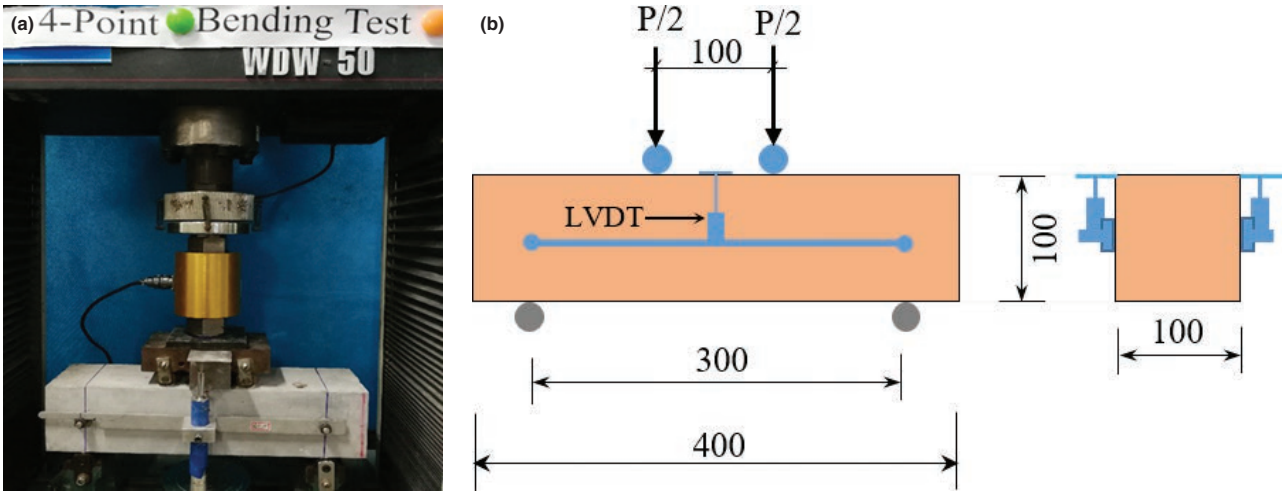

FIGURE 5. Loading setup of the beams. Four-point bending during testing; Schematic diagram.

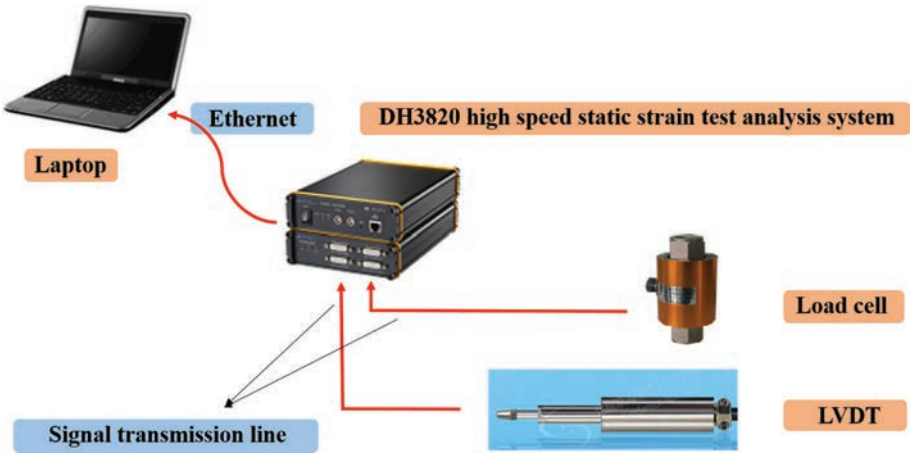

FIGURE 6. Schematic diagram of data collection.

TABLE 5. The result of compressive/ ultimate flexural strengths and its relative increase rates.

		Compressive strength	Relative increase rates on compressive strength			Ultimate flexural strength	Relative increase rates on ultimate flexural strengths		
	Group	f_{cu} (MPa)	$(f_{cu,r}-f_{cu,p})/f_{cu,p}$ (%)	$(f_{cu,f}-f_{cu,s})/f_{cu,s}$ (%)	$(f_{cu,h\text{-}T}-f_{cu,h\text{-}D})/f_{cu,h\text{-}D}$ (%)	f_m (MPa)	$(f_{m,r}-f_{m,p})/f_{m,p}$ (%)	$(f_{m,r}-f_{m,s})/f_{m,s}$ (%)	$(f_{m,h\text{-}T}-f_{m,h\text{-}D})/f_{m,h\text{-}D}$ (%)
Control	Plain	43.409	-	-	-	6.654	-	-	-
Control-I	SS2.0	60.454	39.27	-	-	10.050	51.89	-	-
Series-I	SS1.5SP0.5	52.636	21.26	-12.93	-	9.579	44.70	-4.69	-
	SS1.5SP0.4CW1.0	53.330	22.85	-11.78	1.32	10.901	64.90	8.47	13.80
	SS1.25SP0.75	54.036	24.48	-10.62	-	9.817	48.33	-2.32	-
	SS1.25SP0.55CW2.0	60.217	38.72	-0.39	11.44	9.366	41.45	-6.80	-4.81
Series-II	SS1.5LP0.5	57.888	33.35	-4.24	-	9.832	48.57	-2.16	-
	SS1.5LP0.4CW1.0	61.026	40.58	0.95	5.42	11.752	77.91	16.94	19.53
	SS1.25LP0.75	51.482	18.60	-14.84	-	10.125	53.04	0.75	-
	SS1.25LP0.55CW2.0	62.007	42.84	2.57	20.44	11.540	74.67	14.83	13.97
Control-II	LS2.0	48.439	11.58	-	-	11.145	68.63	-	-
Series-III	LS1.5SP0.5	50.478	16.8	4.21	-	13.073	98.10	17.30	-
	LS1.5SP0.4CW1.0	52.233	20.33	7.83	3.48	12.541	89.96	12.52	-4.07
	LS1.25SP0.75	59.184	36.34	22.18	-	11.703	77.16	5.00	-
	LS1.25SP0.55CW2.0	49.466	13.95	2.12	-16.42	15.423	134.02	38.39	31.79
Series-IV	LS1.5LP0.5	49.375	13.74	1.93	-	12.685	92.17	13.82	-
	LS1.5LP0.4CW1.0	56.739	30.71	17.13	14.91	13.055	97.83	17.14	2.92
	LS1.25LP0.75	51.538	18.73	6.40	-	11.992	81.58	7.60	-
	LS1.25LP0.55CW2.0	52.711	21.43	8.82	2.28	15.410	133.82	38.27	28.51

Note: $f_{cu,p}$ represents compressive strength of plain; $f_{cu,s}$ represents compressive strength of samples with single steel fiber; $f_{cu,f}$ represents compressive strength of samples with fibers; $f_{cu,h\text{-}D}$ represent compressive strength of samples with steel-PVA hybrid fibers; $f_{cu,h\text{-}T}$ represent compressive strength of samples with steel-PVA hybrid fibers -$CaCO_3$ whisker. The letters in ultimate flexural strengths have the similar meaning.

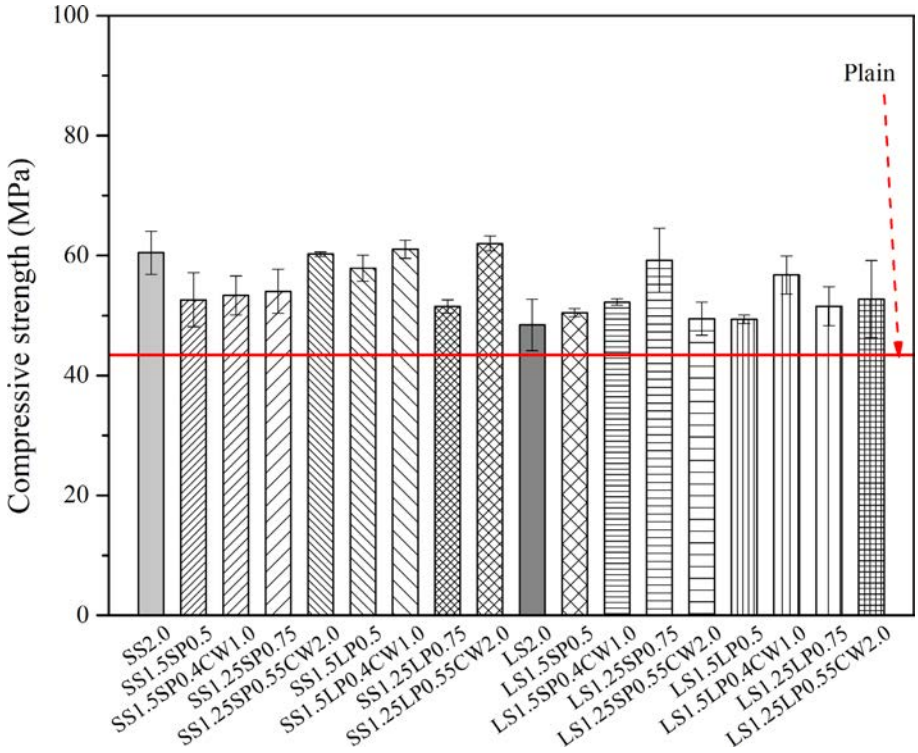

FIGURE 7. Compressive strength of all composites.

12.93%, 10.62%, 4.24% and 14.84%, respectively, as compared to that of SS2.0. The reduction of compressive strength may be due tolow steel fiber content which was replaced by PVA fiber ultimately brought new interfaces. However, a rising trend were observed in LS1.5SP0.5, LS1.5SP0.4CW1.0, LS1.25SP0.75, LS1.25SP0.55CW2.0, LS1.5LP0.5, LS1.5LP0.4CW1.0, LS1.25LP0.75 and LS1.25LP0.55CW2.0 specimens. The reason for increase in compressive strength is very likely the length and content of long steel fibers in LS2.0 which resulted in non-uniform dispersion of long steel fiber in cubes. The compressive strength of SS1.5SP0.4CW1.0, SS1.25SP0.55CW2.0, SS1.5LP0.4CW1.0, SS1.25LP0.55CW2.0, LS1.5SP0.4CW1.0, LS1.5LP0.4CW1.0, LS1.25LP0.55CW2.0 were increased by 1.32%, 11.44%, 5.42%, 20.44%, 3.48%, 14.91% and 2.28%, as compared to that of SS1.5SP0.5, SS1.25SP0.75, SS1.5LP0.5, SS1.25LP0.75, LS1.5SP0.5, LS1.5LP0.5 and LS1.25LP0.75, respectively. This indicated that addition of CW into PVA-steel fiber specimens could increase compressive strength because micro-sized CW filled pores of matrix and improve the compactibility of cubes (12, 17). However, compared with LS1.25SP0.75, the compressive strength of LS1.25SP0.55CW2.0 was decreased by 16.4%which is probably related to discreteness of compression test. Furthermore, the cubes of series-II showed overall higher compressive strength than that of series-I, series-III and series-IV. The SS1.25LP0.55CW2.0 showed highest compressive strength of 62.0 MPa.

4.2. Ultimate flexural strength

The results of ultimate flexural strength of beams are presented in Table 5 and Figure 8. The plain group had lowest flexural strength and its ultimate flexural strength was only 6.65 MPa. The ultimate flexural strength of SS2.0 and LS2.0 were increased by 51.89% and 68.63%, respectively,as compared to that of plain group. This is because presence of steel fiber could effectively control generation and development of crack by bridging effect. Compared to SS2.0, the ultimate flexural strength of SS1.5SP0.5, SS1.25SP0.75 and SS1.5LP0.5 were decreased by 4.69%, 2.32% and 2.16%, respectively, but decreasing trend was not significant. The reason for decrease is weak interface between fibers and matrix caused by addition of PVA fibers. However, SS1.5SP0.4CW1.0, SS1.5LP0.4CW1.0 and SS1.25LP0.55CW2.0 leaded upto 16.94% increment in ultimate flexural strength. The reason may be that CW could improve compactibility of matrix which improves bonding capacity between fibers and matrix.Similarly, ultimate flexural strength of LS1.5SP0.4CW1.0, LS1.25SP0.55CW2.0, LS1.5LP 0.4CW1.0 and LS1.25LP0.55CW2.0 were increased by 12.52%, 38.39%, 17.14% and 38.27%, respectively, as compared to that of LS2.0. The results

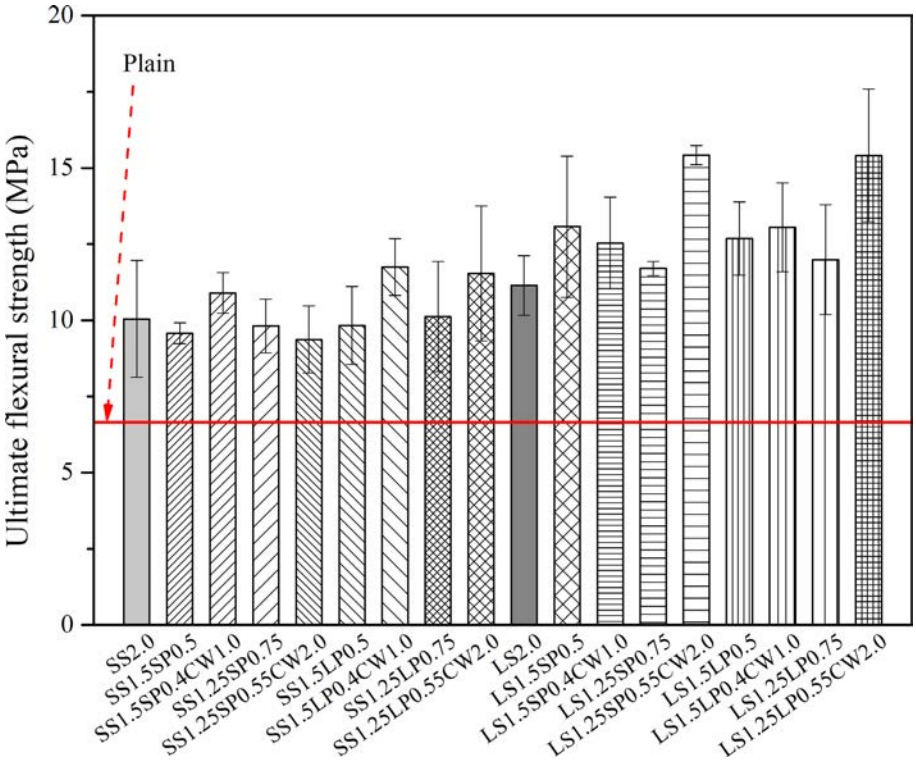

FIGURE 8. Ultimate flexural strength of all composites.

further verified that multiscale hybrid fiber system could improve ultimate flexural strength. The improvement effect came from cracking resistance of $CaCO_3$ whisker-PVA-steel fibers at multi scales such as micron-sized CW, meso PVA fibers and macro steel fibers could delay generation, propagation and development of cracks at micro, meso and macro level, respectively (16, 18). However, SS1.25SP0.55CW2.0 and LS1.5SP0.4CW1.0 were decreased by 4.81% and 4.07%, respectively, as compared to SS1.25SP0.75 and LS1.5SP0.5, respectively. The decrement in ultimate flexural strength of SS1.25SP0.55CW2.0 and LS1.5SP0.4CW1.0could be caused by poor dispersion of some of CW which agglomerate and caused matrix defects. Moreover, it can be seen that the ultimate flexural strength of series-III andseries-IV were higher than that of series-I and series-II. This indicates that long steel fiber had morecontribution to ultimate flexural strength, as compared to that of short steel fiber. The LS1.25SP0.55CW2.0 showed highest ultimate flexural strength of 15.4 MPa.

4.3. Flexural behavior

4.3.1. Flexural response

The load-deflection curves of all composites are shown in Figure 9. The plain group presented typical brittle fracture characteristic and had lowest flexural load and deflection capacity. On the other hand, samples with fibers showed significant ductile failure characteristics and had better load carrying and deformation capacity than that of plain group. The samples consisting of PVA-steel fibers showed extended softening behavior than that of samples with single steel fiber. This behavior could be attributed to cracking resistance effect of PVA and steel fibers at meso- and macro-scales, respectively. The flexural response of PVA-steel fiber specimens was further increased with addition of CW which provided cracking resistance effect at micro-scale.

The flexural parameters at five specific points (first crack, peak load, L/600, L/150 and L/100 points) described in ASTM standards were used to describe flexural behavior of MHFRCC. It can be seen from Table 6 that samples consisting of fibers had better flexural behavior than plain group. The first crack deflection (δ_0) of CW-PVA-steel fibers specimens were higher than that of respective PVA-steel fibers specimens. This indicated that CW contribute to inhibit the generation of microscale crack and improve crack resistance before first cracking. The peak load deflection (δ_m) of samples having CW-PVA-steel fibers were about 1.5 to 12.0 times higher than plain group because CW-PVA-steel fibers system could arrest cracks at multiscale before peak load. For instance, micron-sized CW could inhibit generation and evolution of small

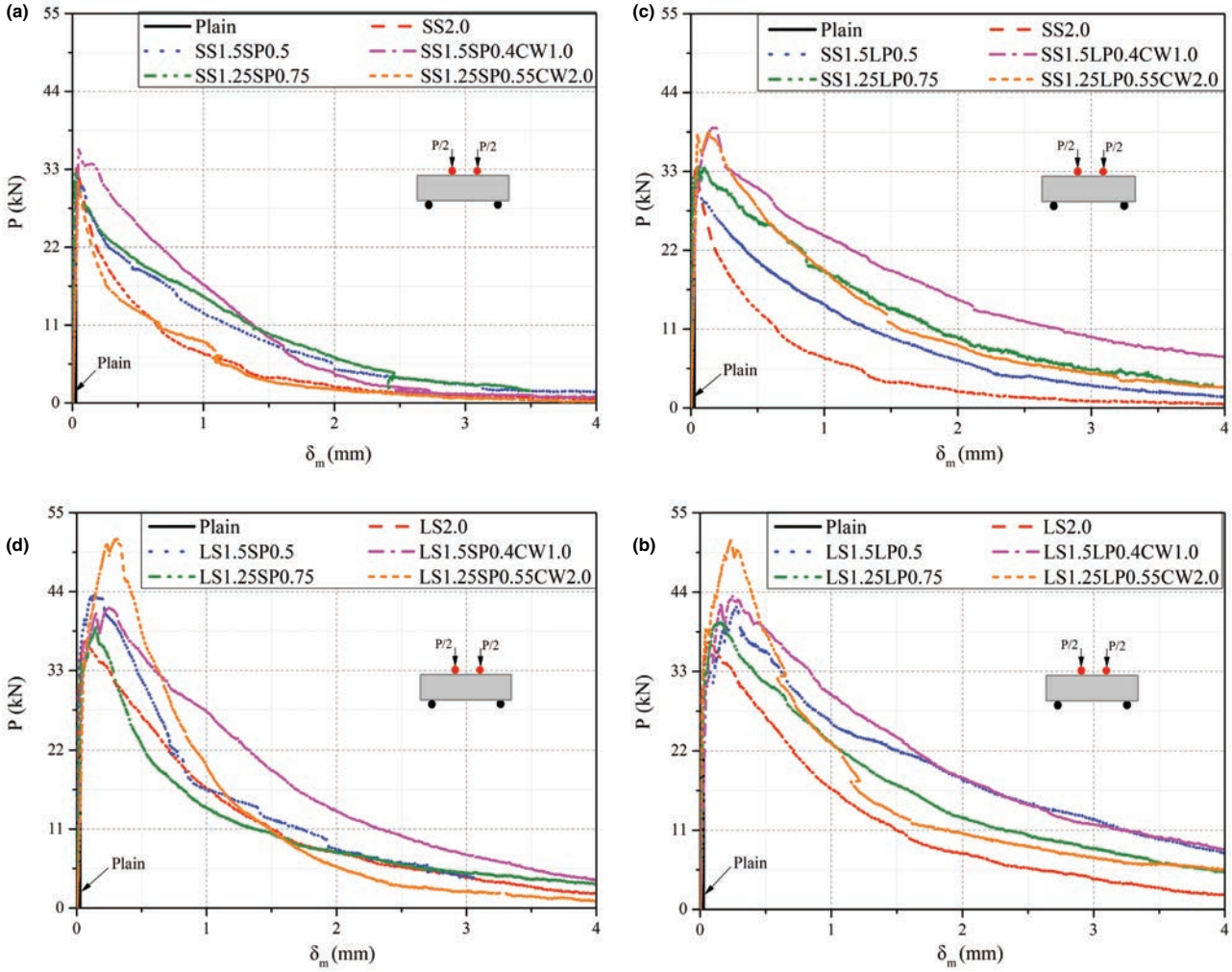

FIGURE 9. Load-deflection curves of all composites. Load-deflection curves of series-I; Load-deflection curves of series-II; Load-deflection curves of series-III; Load-deflection curves of series-IV.

cracks at micro-scale, PVA fiber played an effect role by preventing extension of cracks and decentralized cracks at mesoscale and steel fiber could control cracks by fiber bridging at macroscale. After peak load, with increase in deflection, the residual flexural strength ($f_{L/600}$, $f_{L/150}$ and $f_{L/100}$) began to decrease gradually. It was worth noting that order for residual flexural strength of samples were series-IV followed by series-III, series-II and series-I. The result showed that long steel fibers play a key role after peak load stage because long steel fibers could arrest macro-cracks and hooked ends shape could improve the mechanical anchoring capacity between long steel fibers and matrix. Furthermore, this also indicated that long PVA fiber exhibited a better crack arresting capacity than short PVA fiber in post-peak stage because length of long PVA fiber will be more effective as crack width increases.

4.3.2. Flexural toughness

Toughness is defined as energy absorption capacity of test specimens.The flexural toughness could be obtained by calculating area under the load-net deflectioncurve up a specified deflection according to ASTM C1018-97. The results of flexural toughness at five specific points are presented in Table 6. The flexural toughness of FRCC groups wereremarkably higher than that of plain. Compared to single steel fiber specimens, the samples consising of hybrid fibers brought dramatically improvement in flexural toughness. Figure 10 show the flexural toughness of different samples. It can be seen that flexural toughness of CW-PVA-steel fiberspecimens were higher than that of their respective PVA-steel fiberspecimens at first crack point. This may bedue to addition of CW which act as a filler and improve the compactibility of matrix,

TABLE 6. Flexural parameters of MHFRCC.

Group	First crack point			Peak load point		
	δ_0 (mm)	f_0 (MPa)	T_0 (N·m)	δ_m (mm)	f_m (MPa)	T_m (N·m)
Plain	0.014	4.562	0.133	0.025	6.654	0.332
SS2.0	0.016	6.554	0.241	0.032	10.050	0.691
SS1.5SP0.5	0.022	7.314	0.242	0.036	9.579	0.660
SS1.5SP0.4CW1.0	0.036	8.224	0.449	0.046	10.901	0.782
SS1.25SP0.75	0.017	9.136	0.386	0.020	9.817	0.481
SS1.25SP0.55CW2.0	0.037	7.950	0.485	0.039	9.366	0.534
SS1.5LP0.5	0.026	5.836	0.273	0.040	9.832	0.626
SS1.5LP0.4CW1.0	0.029	6.977	0.323	0.174	11.752	5.447
SS1.25LP0.75	0.017	9.590	0.483	0.054	10.125	1.663
SS1.25LP0.55CW2.0	0.042	9.944	0.687	0.132	11.540	3.989
LS2.0	0.011	8.793	0.210	0.068	11.145	2.173
LS1.5SP0.5	0.013	8.890	0.271	0.131	13.073	4.932
LS1.5SP0.4CW1.0	0.047	11.096	0.874	0.245	12.541	8.595
LS1.25SP0.75	0.033	10.154	0.634	0.147	11.703	4.718
LS1.25SP0.55CW2.0	0.053	10.212	0.799	0.299	15.423	11.898
LS1.5LP0.5	0.026	8.804	0.476	0.282	12.685	9.731
LS1.5LP0.4CW1.0	0.045	9.365	0.638	0.247	13.055	8.503
LS1.25LP0.75	0.025	8.588	0.399	0.152	11.992	5.082
LS1.25LP0.55CW2.0	0.026	10.575	0.609	0.232	15.410	9.697

Group	*Ll*600 point			*L*/150 point			*L*/100 point		
	δ_{Ll600} (mm)	f_{Ll600} (MPa)	T_{Ll600} (N·m)	δ_{Ll150} (mm)	f_{Ll150} (MPa)	T_{Ll150} (N·m)	δ_{Ll100} (mm)	f_{Ll100} (MPa)	T_{Ll100} (N·m)
Plain	-	-	-	-	-	-	-	-	-
SS2.0	0.500	4.122	9.591	2.000	0.696	18.574	3.000	0.294	20.088
SS1.5SP0.5	0.500	5.675	11.500	2.000	1.460	28.253	3.000	0.785	31.853
SS1.5SP0.4CW1.0	0.500	7.533	14.482	2.000	1.284	34.433	3.000	0.377	36.624
SS1.25SP0.75	0.500	6.018	12.110	2.000	1.952	31.011	3.000	0.800	35.115
SS1.25SP0.55CW2.0	0.500	3.907	9.023	2.000	0.572	17.975	3.000	0.239	19.235
SS1.5LP0.5	0.500	6.089	12.189	2.000	1.971	30.763	3.000	0.959	35.246
SS1.5LP0.4CW1.0	0.500	9.217	16.335	2.000	4.523	49.119	3.000	2.969	61.278
SS1.25LP0.75	0.500	7.857	14.913	2.000	2.939	40.458	3.000	1.587	47.718
SS1.25LP0.55CW2.0	0.500	8.374	16.120	2.000	2.611	40.487	3.000	1.419	46.845
LS2.0	0.500	7.999	15.941	2.000	2.312	37.908	3.000	1.274	43.761
LS1.5SP0.5	0.500	9.484	19.117	2.000	2.446	43.203	3.000	1.359	49.413
LS1.5SP0.4CW1.0	0.500	10.616	18.427	2.000	4.054	53.401	3.000	2.233	63.536
LS1.25SP0.75	0.500	6.823	15.472	2.000	2.373	34.655	3.000	1.458	40.834
LS1.25SP0.55CW2.0	0.500	11.495	21.009	2.000	1.716	46.217	3.000	0.697	49.673
LS1.5LP0.5	0.500	10.751	17.887	2.000	5.419	54.977	3.000	3.769	69.877
LS1.5LP0.4CW1.0	0.500	11.701	18.857	2.000	5.449	59.707	3.000	3.531	74.324
LS1.25LP0.75	0.500	9.463	17.295	2.000	3.812	48.326	3.000	2.550	58.703
LS1.25LP0.55CW2.0	0.500	11.550	21.779	2.000	3.169	50.607	3.000	2.163	59.333

thereby enhancing crack resistance before first cracking.Furthermore, CW and PVA fiber of high aspect ratio can delay generation and propagation of mircocracks by mechanism of fiber bridging. Also, the same resultswereobserved at peak point (see Figure 10) and LS1.25SP0.55CW2.0 exhibited best flexural toughness at peak point and reached to 11.898 N·m. However, SS1.25SP0.55CW2.0

showeda little difference after peak load point. Compared to SS1.25SP0.75, flexural toughness of SS1.25SP0.55CW2.0 at L/600, L/150 and L/100 points were decreased by 25.5%, 42.0% and 45.2%, respectively. In comparison with other flexural parameters of SS12.5SP0.55CW2.0 before peak load, it could be concluded that poor dispersion of hybrid fibers resulted in weak flexural behavior. In addition to this, the main energy absorption capacity wastaken from peak load to L/150 deflection as shown in Figure 10. This demonstrated that strain hardening behavior was beneficial to increase energy absorption capacity of samples.

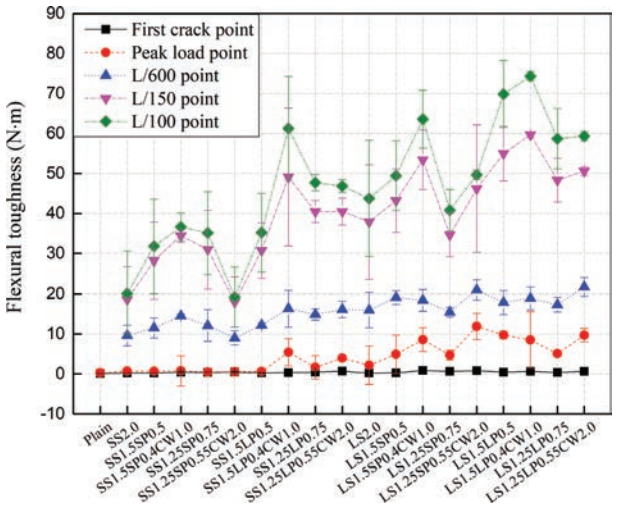

FIGURE 10. Flexural toughness of all composites.

TABLE 7. Post-crack strength and reinforcing index.

Group	Post-crack strength (MPa)			
	PCS_{600}	PCS_{150}	PCS_{100}	RI_v
Plain	0.00	0.00	0.00	0.00
SS2.0	5.71	2.73	1.96	1.30
SS1.5SP0.5	7.01	4.22	3.16	1.48
SS1.5SP0.4CW1.0	9.05	5.17	3.64	1.82
SS1.25SP0.75	7.27	4.63	3.49	1.57
SS1.25SP0.55CW2.0	5.52	2.67	1.90	2.25
SS1.5LP0.5	7.54	4.61	3.51	1.98
SS1.5LP0.4CW1.0	10.02	7.18	5.93	2.22
SS1.25LP0.75	8.91	5.98	4.69	2.32
SS1.25LP0.55CW2.0	9.88	5.86	4.48	2.80
LS2.0	9.55	5.55	4.26	2.11
LS1.5SP0.5	11.52	6.14	4.65	2.32
LS1.5SP0.4CW1.0	11.57	7.66	5.98	2.81
LS1.25SP0.75	9.14	4.85	3.80	2.42
LS1.25SP0.55CW2.0	13.57	6.05	4.20	3.41
LS1.5LP0.5	11.20	7.90	6.64	3.05
LS1.5LP0.4CW1.0	12.28	8.76	7.17	3.40
LS1.25LP0.75	10.53	7.02	5.65	3.51
LS1.25LP0.55CW2.0	13.53	6.94	5.38	4.21

Furthermore, *PCS* technique was also used to evaluate flexural toughness of samples. In this study, *m* wastaken as 600, 150 and 100 to describe flexural toughness. So, the value of *L*/*m*for L/600, L/150 and L/100 were 0.5, 2 and 3 mm, respectively. The aimto select these *L*/*m*values wereto maintain consistency with the evaluation of flexural toughness based on ASTM standards. It can be seen from Table 7 and Figure 11 that *PCS* values at small deflection werehigher than that of large deflection. The tendency of fluctuations at 0.5 mm were different from that of 2 mm and 3mm which is due tocrack bridging effect of PVA-steel fibers at 0.5mm. However, only steel fibers affected cracking behavior at 2 mm and 3 mm. The LS1.25SP0.55CW2.0 and LS1.25LP0.55CW2.0 hada higher *PCS* values than others when *L*/*m* equal to 0.5 mm. Moreover, *PCS* loss rate was also relatively higher when *L*/*m* equal to 2 mm and 3 mm. The resaon maybe due to low content of long steel fibers. For instance, samples consising of 1.5 vol % of steel fiber, 0.4 vol % PVA fiber and 1.0 vol % of CW (SS1.5SP0.4CW1.0, SS1.5LP0.4CW1.0, LS1.5SP0.4CW1.0 and LS1.5LP0.4CW1.0) had highest *PCS* in their respective series. This indicated that steel fibers with 1.5 vol% contents improved post-peak behavior at a larger deflection more efficiently. With increasein crack width, long steel fibers had a better bridging capability than that of short steel fibers. However, it is also need to pointed out that decreased *PCS* was not only related to the geometrical shape size and content of fibers but also in connection with location and characteristic of cracks.

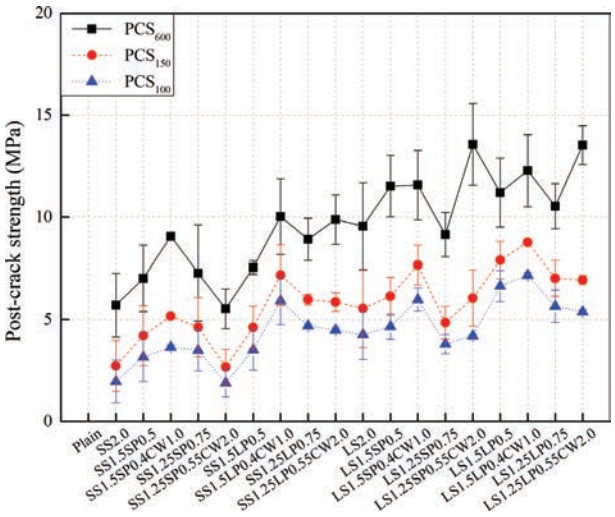

FIGURE 11. Post-crack strength of all composites.

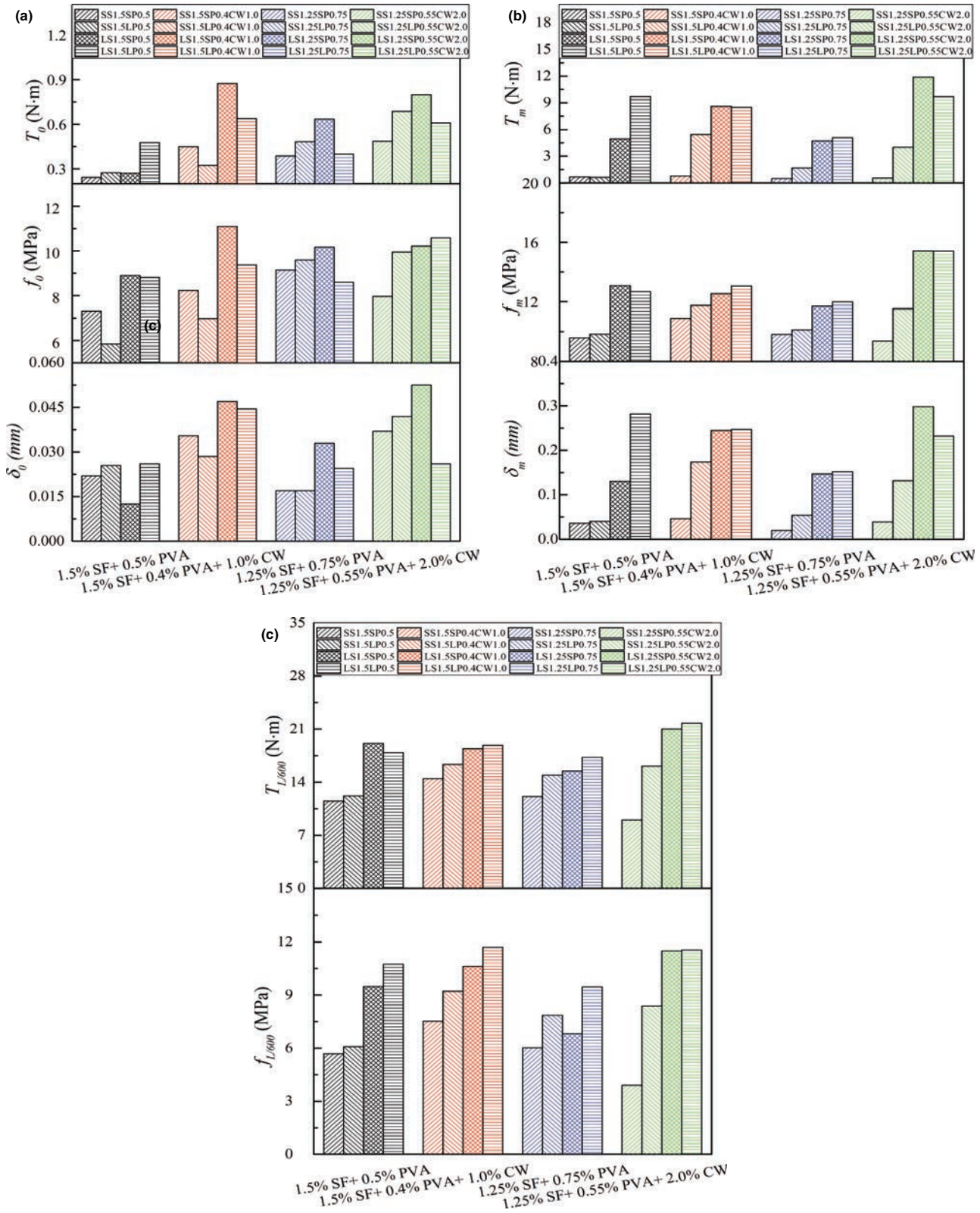

FIGURE 12. Variation of the flexural parameters with respect to fiber content. (Note: SF represents steel fiber, PVA represents PVA fibers and CW represents $CaCO_3$ whisker). Flexural parameters at first cracking point; Flexural parameters at maximum load point; Flexural parameters at L/600 deflection point; Flexural parameters at L/150 deflection point; Flexural parameters at L/100 deflection point.

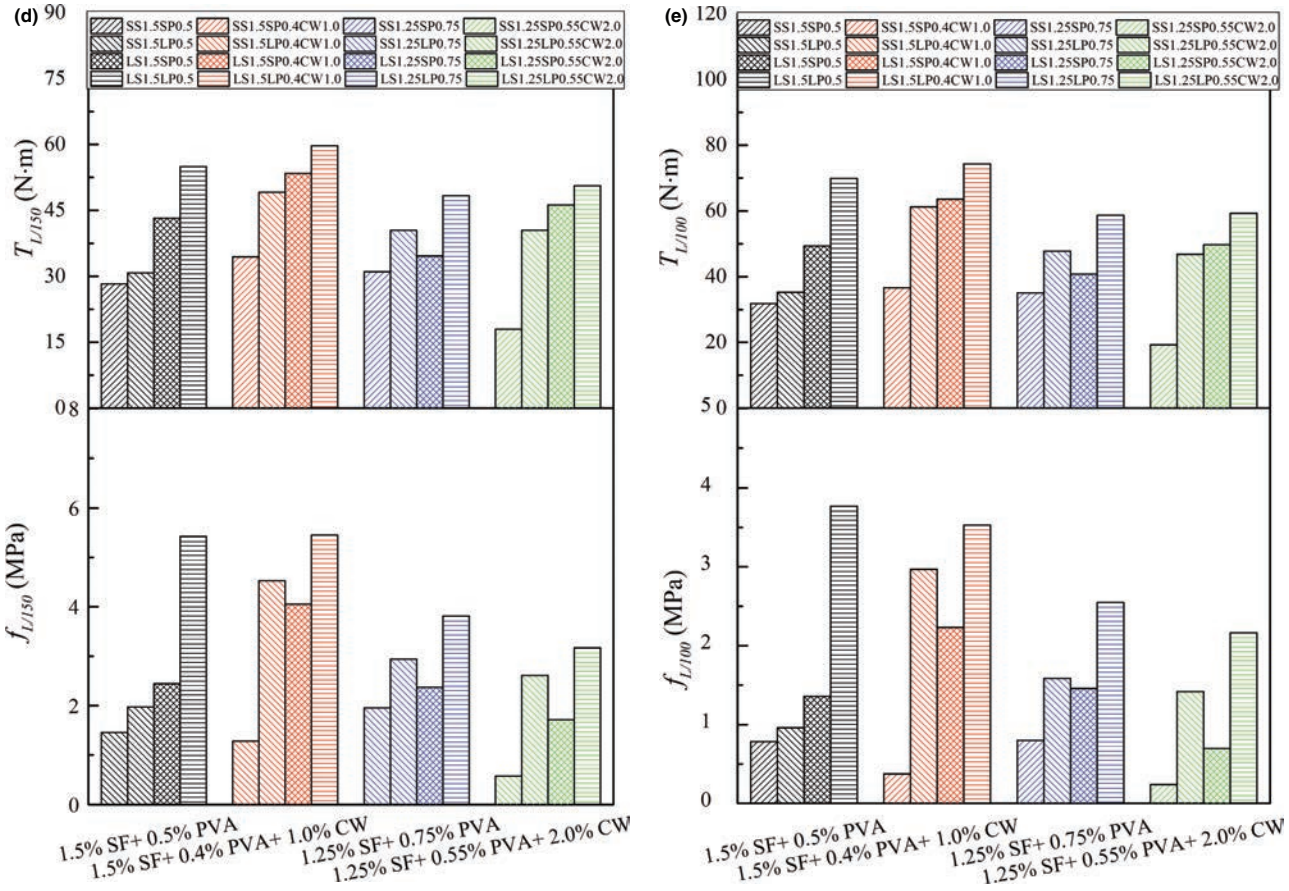

FIGURE 12. (Continued) Variation of the flexural parameters with respect to fiber content. (Note: SF represents steel fiber, PVA represents PVA fibers and CW represents $CaCO_3$ whisker). Flexural parameters at first cracking point; Flexural parameters at maximum load point; Flexural parameters at L/600 deflection point; Flexural parameters at L/150 deflection point; Flexural parameters at L/100 deflection point.

4.3.3. Influence of different fiber combination on flexural behavior

The flexural parameters with different fiber combination are illustrated in Figure 12. At first cracking points, the hybrid fiber combination of LS+SP+CW significantly improved deflection capacity (δ_0), flexural strength (f_0) and flexural toughness (T_0) of cement-based materials. The LS1.5SP0.4CW1.0 and LS1.25SP0.55CW2.0 exhibited a better flexural behavior than that of other samples. The excellent flexural behavior at first cracking points may be due to hybrid effect of short PVA fiber and CW which could inhibit cracks at micro-meso scales before first cracking. Also, the long steel fiber could disperse easily at the same content ascompared to short steel fiber due to its less quantity. When the flexural strength reach peak, the samples consising of LS+SP+CW still showed a good flexural behavior. The deflection capacity (δ_m), flexural strength (f_m) and flexural toughness (T_m) of LS1.25SP0.55CW2.0 was 0.299 mm, 15.423 MPa and 11.898 N·m, respectively. However, the crack resistance capacity of CW and short PVA fibers decreased gradually with increase in crack width which is likely due to the limition of its small length. Moreover, at the same time long steel fibers and long PVA fibers started to play a bridging role to control cracks at macro level. Thus, it can be seen from Figue 12 (c), 12 (d) and 12 (e) that the hybrid fiber combination of LS+LP+CW showed a higher flexural properties, especially LS1.5LP0.4CW1.0 presented highest flexural toughness.

Moreover, the flexural behavior is also in connection with hybrid fiber contents. The LS1.25SP0.55CW2.0 showed higher flexural parameters before L/600 deflection as compared to that of others samples. The 1.25 vol % of long steel fiber, 0.55 vol % of short PVA fiber and 2.0 vol % of CW was considered as the optimium fiber combination before L/600 deflection. However, LS1.5LP0.4CW1.0 exhibited a better flexural behavior after L/600 deflection and 1.5 vol % of long steel fibers, 0.4 % of long PVA fibers and 1.0 % of CW was taken as the optimium fibers combination.

4.3.4. Crack behavior

The crack behavior of all composites are presented in Figure 13. It can be seen that fractures of all samples demonstrated one major crack. The plain specimen was broken into two parts but FRCC was still connected by fibers dueto the effect of fiber bridging. However, more secondary cracks were observed in CW-PVA-steel fiber specimensas compared to that of PVA-steel fiber specimens. This is consistent with the results of flexural toughness. The resaon maybe due to the crack arresting mechanismof steel fiber, PVA fiber and CW at macro-, meso- and micro-scales, respectively. Thus, it could be concluded that multiple cracking behaviors may contributes towards improved energy absorption capacity.

4.4. Correlation between reinforcing index and flexural behavior

The hybrid fiber type, length and content are significant material parameters affecting the flexural behavior of beams. Thus, it is necessary to synthesize these materials parameters to describe characteristics of hybrid fibers. The comprehensive reinforcing index (RI_v) was a suitable parameter used by Almusallam et al. (24) and Cao (29). In this study, RI_v values were calculate by Equation. (4) and the resultsare shown in Table 7. The relationship between RI_v and flexural parameters of beams are shown in Figure 14. A linear relationship between RI_v and flexural parameters was developed and the trend of fitted linesshowed that the flexural parameters increases with the increase in RI_v. Furthermore, a slightly increase in first cracking deflection was observed with the increase in RI_v (see Figure 14(a). There as on is because the samples seems to be more elastic with the decreased modulus of elasticity asRI_v increases (22, 23). The fitted curve of δ_m showeda significant increment of deflection at ultimate load as RI_v increases. This indicates that addition of hybrid fiber brought significantly improvement in deformability of cement-based materials. The linear fitting results for deflection can reasonably reflect the regularity of deflection variation with increasing of RI_v.Figure 14 (b) demonstrated that theincreased RI_vcan provide a

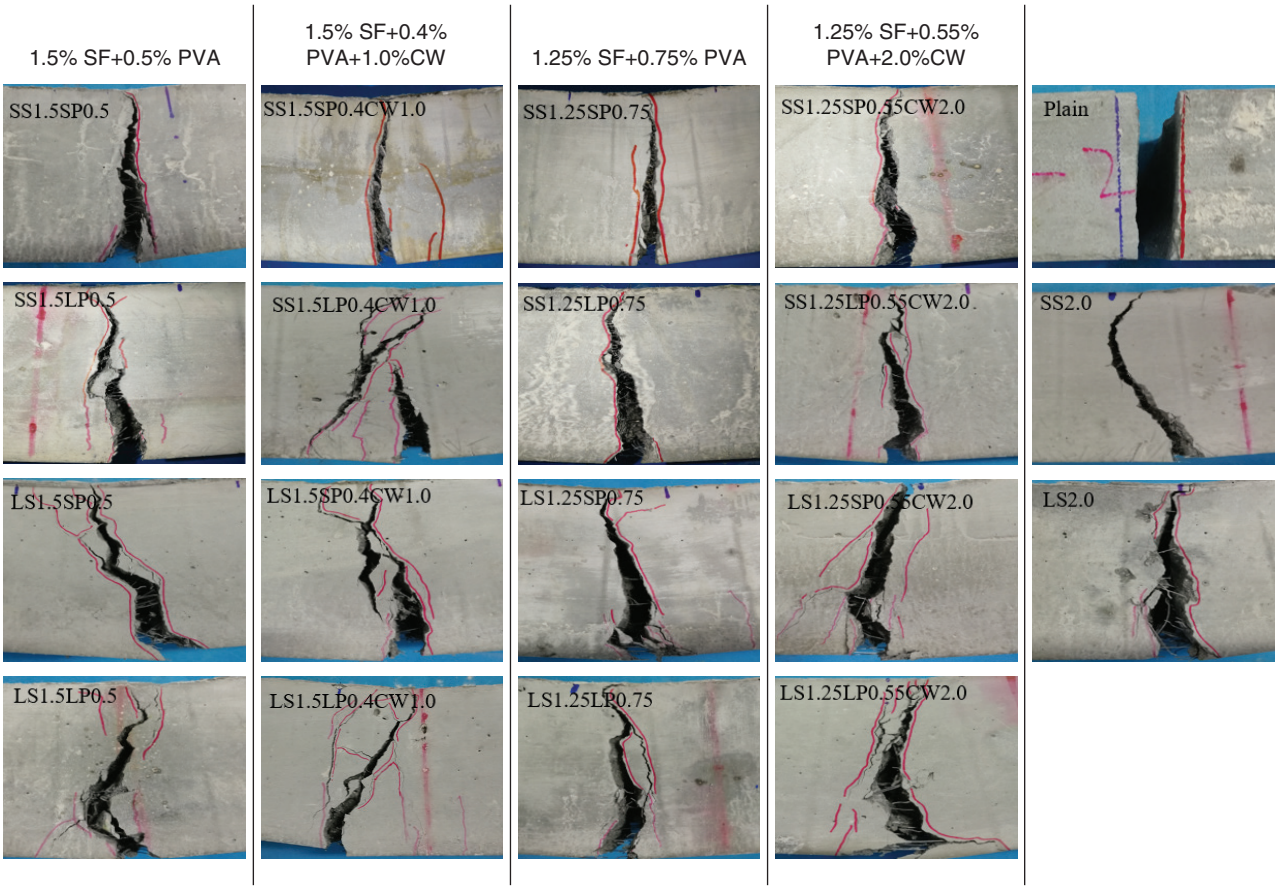

FIGURE 13. Crack pattern of all composties.

better load carrying capacity. In particularly, as RI_v increases, the increment in trendency of $f_{L/600}$ were more obvious than others (f_0, f_m, $f_{L/150}$ and $f_{L/100}$). Figure 14 (c) showed that the flexural toughness were plotted with increasing RI_v. The increamentin RI_v results in increased flexural toughness and all of the fitted curves for flexural toughness was found to be linear. The slope of fitted curves for T_0 was almost parallel to x-axis. The reason maybe that only micron-sized CW and some of short-sized PVA fibers were playedan effectiverole in crack arresting before first cracking. Later, the cracks was extensively propagated as loading increased and the hybrid fibers began to work there by improving energy absorption capability. Thus, the increase in flexural toughness at large deflection was more evident than that at first cracking deflection. It can be seen from Figure 14 (d) that the general trend of these results seems to be directly proportional to RI_v value according to the linear fit of PCS. The increased PCS indicated a better energy absorption capability of samples as RI_v increased. The resluts showed a good consistency with the flexural parameters described in ASTM C1609.

5. DISCUSSION

The PVA-steel fibers-CW specimens showed a better compressive strength and flexural behavior than that of their respectivesteel-PVA fiber specimens. The SS1.25LP0.55CW2.0 exhibited highest compressive strength.The compressive strength of SS1.25LP0.55CW2.0 was increased by 42.9%, as compared to that of plain specimen. This is because 2.0 vol % of CW could maximum fill poresand improved compactibility of matrix.The

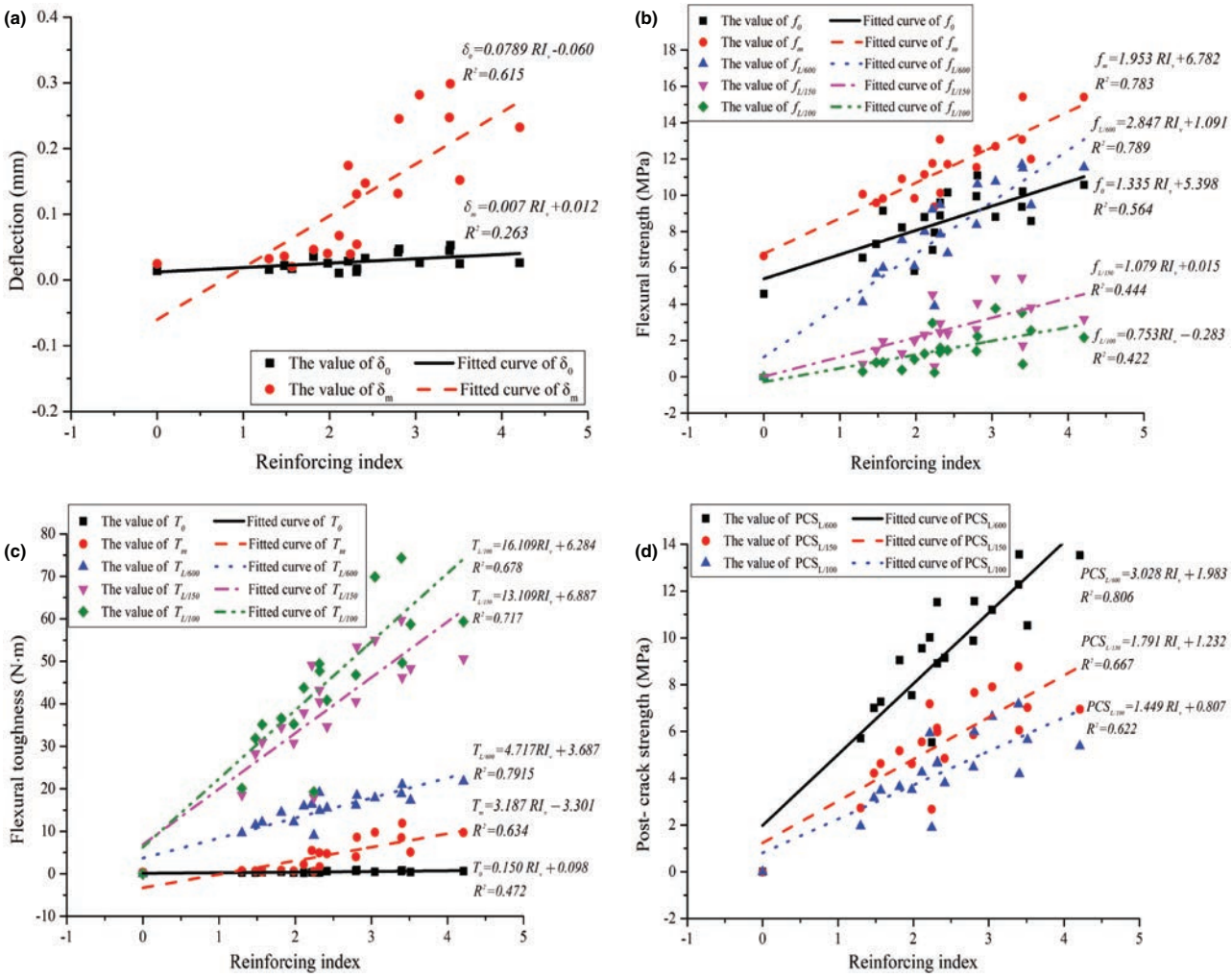

FIGURE 14. The relationship between RIv vs flexural parameters. Correlation between RI_v vs deflection (δ); Correlation between RI_v vs flexural strength (f); Correlation between RI_v vs flexural toughness (T); Correlation between RI_v vs post-crack strength (PCS).

ultimate flexural strength of LS1.25SP0.55CW2.0 was increased by134% than that of plain specimen. Meanwhile, LS1.25SP0.55CW2.0 exhibited highest flexural toughness before *L*/600 deflection. This can be attributed to the crack arresting effect of 1.25 vol % LS, 0.55 vol % of SP and 2 vol % of CW atmacro-, meso- and micro-scales before peak load. Moreover, the LS1.5LP0.4CW1.0 showed highest residual strength and flexural toughness at *L*/150 and *L*/100 deflections with increase in crack width which is probably because of long PVA fiberbridging effect at large deflection. Compared to LS1.5LP0.4CW1.0, the residual strength and flexural toughness of LS1.25LP0.55CW2.0 wereless at *L*/150 and *L*/100 deflections. The reason maybe due to more long steel fibers and long PVA fibers contents which arrest cracks at large deflection. The *PCS* results also indicated that LS1.25SP0.55CW2.0 had a better energy absorption capability, i.e.13.6 MPa than other specimens at *L*/600 deflection. The LS1.5LP0.4CW1.0 showed highest *PCS* value at *L*/150 and *L*/100 deflections.Thus, the evaluation results on flexural toughness based on *PCS* technique had good consistency with the calculated results based on ASTM standards.The crack pattern of PVA-steel fibers-CW specimens showed more amounts of cracks on the side of beams(especially, LS1.25SP0.55CW2.0 and LS1.5LP0.4CW1.0) which indicated that the occurrence of multiple cracks could consume more energy. Moreover, poor dispersibility of fibers can account for the weak flexural behavior.The relationship between comprehensive reinforcing index (RI_v) and flexural parameters indicated that there existed a linear relation. Also, the trend of fitted lines between $RI_v$and flexural parameters showed that the flexural parameters increases with increase in RI_v. The comparative flexural behavior of hybrid FRCCs with different CW, PVA-steel fiber content and length can further comprehensively understand in structural applications. The optimized CW and PVA-steel fiber content and length are favoring it utility for improving performance of flexural members.

6. CONCLUSIONS

The flexural deflection capacity (δ), strength (f), toughness (T) and post-crack strength (PCS) were determined to evaluate flexural behavior of multiscale fibers reinforced cementitious composites (MHFRCC).The inflence of different PVA-steel fiber length and contenton $CaCO_3$ whisker reinforced cementitious composites were discussed. The following conclusions were made:

- The SS1.25LP0.55CW2.0 showed a better compressive strength due to the addition of $CaCO_3$ whiskers which increased the compactness of matrix and improved interfaces between PVA-steel fiber and matrix. Meanwhile, well-dispersed PVA-short steel fibers (SS) were beneficial to restrain the development of cracks.
- The LS1.25SP0.55CW2.0 exhibited best flexural behavior before *L*/600 deflection which was because of 2.0 vol % $CaCO_3$ whiskers and 0.55 vol % short PVA fibers (SP) that provided the best crack resistance effect at micro-meso scale. Also, 1.25 vol % long steel fibers (LS) could effectively bridge cracks at macroscopic level. However, LS1.5LP0.4CW1.0 presented best flexural behavior because of 0.4 vol % long PVA fibers (LP) provided bridging effect with 1.5 vol % long steel fibers (LS) at large deflections of L/150 and L/100.
- The *PCS* results showed good consistency with the evaluated results based on ASTM standards. The LS1.25SP0.55CW2.0 had highest *PCS* value at *L*/600 deflection but *PCS* of LS1.5LP0.4CW1.0 transcendedLS1.25SP0.55CW2.0at *L*/150 and *L*/100 deflections which indicated that high contents and long-sized steel-PVA fibers provided bettter bridging effect at large deflection.
- The reinforcing indiex (RI_v) and flexural parameters showed a linear relationship and trend of the fitted lines demonstrated that flexural parameters increases with increasein RI_v.

Hence, the optimized $CaCO_3$ whiskers, PVA and steel fiber length and content are favoring its utility for structural application. The hybrid fibers combination of LS1.25SP0.55CW2.0 and LS1.5LP0.4CW1.0 can be helpful in improving flexural performance of beams.

ACKNOWLEDGMENT

The authors would like to acknowledge the support of this work by Natural Science Foundation of China under Grant No.51678111 and No.51478082. The authors are also thankful to China Scholarship Council (CSC) for providing financial support for PhD studies of Engr. Mehran Khan at Dalian University of Technology, Dalian, China.

REFERENCES

1. Banthia, N.; Trottier, J. F. (1995) Test methods for flexural toughness characterization of fiber reinforced concrete: some concerns and a proposition. *ACI Mater. J.*92, 48–48.
2. Biolzi, L.; Cattaneo, S.; Guerrini, G. L. (2000) Fracture of plain and fiber-reinforced high strength mortar slabs with EA and ESPI monitoring. *Appl. Compos. Mater.* 7[1], 1–12. https://doi.org/10.1023/A:1008948125654
3. Bencardino, F.; Rizzuti, L.; Spadea, G.; Swamy, R. N. (2010) Experimental evaluation of fiber reinforced concrete fracture properties. *Compos. Part B-Eng,* 41[1], 17–24. https://doi.org/10.1016/j.compositesb.2009.09.002
4. Kizilkanat, A. B. (2016) Experimental Evaluation of Mechanical Properties and Fracture Behavior of Carbon Fiber Reinforced High Strength Concrete. *Period. Polytech-Civ.* 60(2), 289. https://doi.org/10.3311/ppci.8509

5. Maekawa, K.; Ishida, T.; Kishi, T. (2003) Multi-scale modeling of concrete performance. *J. Adv. Concr. Technol.* 1(2), 91–126. https://doi.org/10.3151/jact.1.91
6. Pereira, E. B.; Fischer, G.; Barros, J. A. (2012) Effect of hybrid fiber reinforcement on the cracking process in fiber reinforced cementitious composites. *Cem. Concr. Comp.* 34[10], 1114–1123. https://doi.org/10.1016/j.cemconcomp.2012.08.004
7. Banthia, N.; Soleimani, S. M. (2005) Flexural response of hybrid fiber-reinforced cementitious composites. *ACI Mater. J.* 102(6), 382–389. https://doi.org/10.14359/14800
8. Qian, C. X.; Stroeven, P. (2000) Development of hybrid polypropylene-steel fibre-reinforced concrete. *Cem.Concr. Res.* 30[1], 63–69. https://doi.org/10.1016/S0008-8846(99)00202-1
9. Ding, Y.; Zhang, Y.; Thomas, A. (2009) The investigation on strength and flexural toughness of fibre cocktail reinforced self-compacting high performance concrete. *Constr. Build. Mater.* 23[1], 448–452. https://doi.org/10.1016/j.conbuildmat.2007.11.006
10. Dawood, E. T.; Ramli, M. (2012) Mechanical properties of high strength flowing concrete with hybrid fibers. *Constr. Build. Mater.* 28[1], 193–200. https://doi.org/10.1016/j.conbuildmat.2011.08.057
11. Kim, D. J.; Park, S. H.; Ryu, G. S.; Koh, K. T. (2011) Comparative flexural behavior of hybrid ultra high performance fiber reinforced concrete with different macro fibers. *Constr. Build. Mater.* 25[11], 4144–4155. https://doi.org/10.1016/j.conbuildmat.2011.04.051
12. Cao, M.; Zhang, C.; Wei, J. (2013) Microscopic reinforcement for cement based composite materials. *Constr. Build. Mater.* 40, 14–25. https://doi.org/10.1016/j.conbuildmat.2012.10.012
13. Cao, M.; Zhang, C.; Lv, H.; Xu, L. (2014) Characterization of mechanical behavior and mechanism of calcium carbonate whisker-reinforced cement mortar. *Constr. Build. Mater.* 66, 89–97. https://doi.org/10.1016/j.conbuildmat.2014.05.059
14. Zhang, C.; Cao, M. (2014) Fiber synergy in multi-scale fiber-reinforced cementitious composites. *Journal of Reinforced Plastics and Composites,* 33[9], 862–874. https://doi.org/10.1177/0731684413514785
15. Cao, M.; Zhang, C.; Lv, H. (2014) Mechanical response and shrinkage performance of cementitious composites with a new fiber hybridization. *Constr. Build. Mater.* 57, 45–52. https://doi.org/10.1016/j.conbuildmat.2014.01.088
16. Cao, M.; Zhang, C.; Li, Y.; Wei, J. (2014) Using calcium carbonate whisker in hybrid fiber-reinforced cementitious composites. *ASCE J. Mater. Civ. Eng.* 27[4], 04014139. https://doi.org/10.1061/(ASCE)MT.1943-5533.0001041
17. Cao, M.; Li, L.; Khan, M. (2018) Effect of hybrid fibers, calcium carbonate whisker and coarse sand on mechanical properties of cement-based composites. *Mater. Construcc.* 68[330], e156. https://doi.org/10.3989/mc.2018.01717
18. Cao, M.; Xie, C.; Li, L.; Khan, M. (2018) The relationship between reinforcing index and flexural parameters of new hybrid fiber reinforced slab. *Comput. Concrete.* 22[5], 481–492. https://doi.org/10.12989/cac.2018.22.5.481
19. joo Kim, D.; Naaman, A. E.; El-Tawil, S. (2008) Comparative flexural behavior of four fiber reinforced cementitious composites. *Cem.Concr. Comp.*30[10], 917–928. https://doi.org/10.1016/j.cemconcomp.2008.08.002
20. ASTM C 1018 (1997) Standard test method for flexural toughness and first crack strength of fiber reinforced concrete (using beam with third-point loading), American Society for Testing and Materials; West Conshohocken, PA.
21. ASTM C1609/1609M (2012) Standard test method for flexural performance of fiber-reinforced concrete (using beam with third-point loading), American Society for Testing and Materials; West Conshohocken, PA.
22. Said, S. H.; Razak, H. A.; Othman, I. (2015) Flexural behavior of engineered cementitious composite (ECC) slabs with polyvinyl alcohol fibers. *Constr. Build. Mater.*75, 176–188. https://doi.org/10.1016/j.conbuildmat.2014.10.036
23. Said, S. H.; Razak, H. A. (2015) The effect of synthetic polyethylene fiber on the strain hardening behavior of engineered cementitious composite (ECC). *Mater. Design.* 86, 447–457. https://doi.org/10.1016/j.matdes.2015.07.125
24. Almusallam, T.; Ibrahim, S. M.; Al-Salloum, Y.; Abadel, A.; Abbas, H. (2016) Analytical and experimental investigations on the fracture behavior of hybrid fiber reinforced concrete. *Cem. Concr. Comp.* 74, 201–217. https://doi.org/10.1016/j.cemconcomp.2016.10.002
25. Ibrahim, S. M.; Almusallam, T. H.; Alsalloum, Y. A.; Abadel, A. A.; Abbas, H. (2016) Strain rate dependent behavior and modeling for compression response of hybrid fiber reinforced concrete. *Latin American Journal of Solids & Structures,* 13(9). http://dx.doi.org/10.1590/1679-78252717
26. Ezeldin, A. S.; Balaguru, P. N. (1992) Normal and high-strength fiber-reinforced concrete under compression. *ASCE J. Mater. Civ. Eng.* 4[4], 415–429. https://doi.org/10.1061/(ASCE)0899-1561(1992)4:4(415)
27. Abadel, A. A. (2015) Mechanical properties of hybrid fibre-reinforced concrete – analytical modelling and experimental behaviour. *Mag. Concr. Res.* 68[16], 823–843. https://doi.org/10.1680/jmacr.15.00276
28. CECS38 (2004) Technical specification for fiber reinforced concrete structures, China Association for engineering construction standardization, China Architecture & Building Press; Beijing, China.
29. Cao, M.; Li, L. (2018) New models for predicting workability and toughness of hybrid fiber reinforced cement-based composites. *Constr. Build. Mater.*176, 618–628. https://doi.org/10.1016/j.conbuildmat.2018.05.075
30. CECS13 (2009) Standard test method for fiber reinforced concrete, China Association for engineering construction standardization,China Architecture & Building Press; Beijing, China.
31. GB/T 50081 (2002) Standard for test method of mechanical properties on ordinary concrete, Ministry of Construction, China Architecture & Building Press; Beijing, China.